AN ABSTRACT OF THE THESIS OF

Joan Marie Oylear for the degree of Master of Science

in Nuclear Engineering presented on July 26, 1979

Title: Thermal Hydraulic Analysis of a Pressurized Water Reactor

Redacted for privacy

Abstract approved: K. L. Peddicord

The assurance that departure from nucleate boiling (DNB) does not occur is an important basis for the design and operation of pressurized water reactors. In general, previous analyses of the departure from nucleate boiling ratio (DNBR), specifying the ratio of the heat flux at which DNB occurs to the local heat flux, have been deterministic and conservative. From these analyses it is difficult to assess the probability of attaining a critical value.

An alternative technique has been demonstrated in this analysis which results in a best-estimate calculation of the DNBR and its probability distribution. A computer code, COBRA IIIC/MIT, was used to perform the best-estimate calculation. Additional computer runs were made with the code to perform a sensitivity analysis

on the code input variables in order to identify significant variables and minimize subsequent computational effort. Eight of the input parameters, including the fuel and clad physical properties and the grid spacer loss coefficients, showed no effect upon the calculated DNBR. Four other parameters, system pressure, coolant inlet temperature, and average mass velocity and heat flux, were shown to have an effect on the value of the DNBR. With the less sensitive input variables eliminated, the code was then used to evaluate the DNBR at selected combinations of the significant input parameters as prescribed by a central composite experimental design. The resulting response surface used to represent the functional relationship between the code input and output was determined to be

$$DNBR = 2.7043 + 5.6191 \times 10^{-2} x_1 - 1.2256 \times 10^{-1} x_2 + 1.4939 \times 10^{-1} x_3 - 8.8544 \times 10^{-2} x_4 - 1.4075 \times 10^{-2} x_2^2$$

where x_n represents coded variables defined by

x_1 = (Pressure, psia - 2250.)/45

x_2 = (Coolant temp., °F - 552.5)/5.525

x_3 = (Mass Flow, lb/hr-ft^2 - 2.46 x 10^6)/1.488 x 10^5

x_4 = (Heat Flux, Btu/hr-ft^2 - 1.898 x 10^5)/3.796 x 10^3

The final estimate of the DNBR distribution was determined using a direct Monte Carlo technique in which input values were chosen at random from their respective distributions

and propagated through the response function. From the resulting distribution it was demonstrated that, for the given conditions, the realistic probability of attaining a critical value of a DNBR was acceptably low.

Thermal Hydraulic Analysis of a Pressurized Water Reactor

by

Joan Marie Oylear

A THESIS

submitted to

Oregon State University

in partial fulfillment of
the requirements for the
degree of

Master of Science

Completed July 26, 1979

Commencement June 1980

APPROVED:

Redacted for privacy

Professor of Nuclear Engineering in charge of major

Redacted for privacy

Head of Department of Nuclear Engineering

Redacted for privacy

Dean of Graduate School

Date thesis is presented July 26, 1979

Typed by Robin Keen for Joan Marie Oylear

TABLE OF CONTENTS

LIST OF FIGURES

LIST OF TABLES

THERMAL HYDRAULIC ANALYSIS OF A PRESSURIZED WATER REACTOR

I. INTRODUCTION

A large number of postulated accidents for pressurized water reactors may result in the phenomena of the departure from nucleate boiling (DNB). This is characterized by the sudden deterioration in the heat transfer mechanism, resulting in a significant temperature increase of the heated surface of the fuel rod. An important design basis is the assurance that DNB does not occur. This limit is given by the departure from nucleate boiling ratio (DNBR), defined as the ratio of the heat flux at which DNB is expected to occur to the local reactor heat flux. If the DNBR is greater than one, adequate heat transfer is assured between the fuel rod and the reactor coolant and the possible damage to the fuel cladding is avoided.

Since the DNBR is such an important factor in the operation of a pressurized water reactor, it is of interest to determine how it is affected by variations in the parameters of which it is a function, such as reactor core pressure, coolant inlet temperature, or core flow rate. From a safety standpoint, it would also be useful to obtain a realistic estimate of the probability that the local heat flux will not exceed the critical limit at which DNB occurs.

Analysis methods and correlations have been developed to calculate the DNBR and, hence, verify reactor design features. In general, however, these analyses are deterministic and conservative rather than best-estimate calculations. The parameter values are taken at their respective conservative limits and the resulting DNBR is assumed only to envelop or bound the actual result for any specific case. With such analyses, it is difficult to assess the probability of attaining a critical value of less than one.

As an alternative to the conservative analysis a best-estimate calculation of the DNBR can be made and its probability distribution determined. With such information, the suitability of a design could be demonstrated by showing that the realistic probability of attaining a DNBR less than one is acceptably low.

A best-estimate calculation can be made with a computer code containing a mechanistic physical model of the reactor core and with the nominal values of the input parameters. In principle, it is also possible to obtain the statistical distribution of the DNBR given the statistical distributions of the input parameters, but only after a large number of computer runs. Since the analysis of a nuclear reactor is very complicated and suitable computer codes are complex and time consuming, the acquisition of the DNBR distribution may be quite costly.

It is therefore advantageous to find an inexpensive and efficient method to obtain reasonably accurate estimates of the probabilities without requiring a large number of computer runs.

One method that has been suggested by Mazumdar[1] to eliminate an excessive number of computer runs is to approximate the computer code by a suitable graduating function, called a response surface, and to estimate the probability distribution of the output variable from this fitted function using a Monte Carlo technique. Thus, instead of running the code to make a large number of evaluations of the DNBR resulting from variations in the input parameters, the code is run only a limited number of times, and the resulting data is used to fit an appropriate function which then can be used instead of the computer code in subsequent evaluations.

In this study, the COBRA IIIC/MIT computer code[2] is used as the best-estimate model to calculate the limiting DNBR of a typical four-loop pressurized water reactor. This code determines the steady-state and transient core thermal hydraulic behavior of a reactor by performing a subchannel analysis. A description of the code and its method of solution is included in Chapter II.

Before beginning the analysis to determine the most probable DNBR and its probability distribution, the basic

input data to perform the calculations must be obtained. This includes the input information, such as reactor core pressure or coolant temperature, and the thermal hydraulic parameters and correlations to be used in the code. This information plus the reactor core modeling is described in Chapter III.

To begin the analysis, a sensitivity study must be performed to identify the significant input variables to which DNBR is most sensitive. By determining these important parameters initially, the computational effort due to the relatively insignificant variables can be eliminated while retaining those that will eventually result in an appropriate response surface.

This initial significance screening is completed by using a one-at-a-time design. The DNBR values are plotted as a function of a single input variable while all other parameters are kept fixed. This gives an indication of the relative importance of each of the input variables as well as the form of the response.

When the less significant variables have been eliminated, the code is then used to evaluate the DNBR at selected combinations of the input values, as prescribed by a central composite design which includes interaction effects. After selecting the probable significant interacting input variables, a response surface can be fitted to the data.

Once a suitable function has been found that adequately represents the functional relationship between the code input and the resulting DNBR, the DNBR distribution can be determined using a Monte Carlo technique in which input values are chosen at random from their respective distributions and propagated through the response function. Thus, with a model in the form of a response surface and with the statistical distributions of the significant input variables, it is possible to derive an estimate of the probability that the critical heat flux will be exceeded and DNB will occur.

II. BEST-ESTIMATE MODEL: COBRA IIIC/MIT

2.1 General Description

The COBRA IIIC/MIT computer program has been developed to model the steady state and transient thermal hydraulic behavior of a nuclear reactor core. It is capable of computing the coolant flow and enthalpy along parallel flow channels in a three-dimensional reactor core consisting of rod-bundle fuel elements.

The MIT version of the code is based on an earlier code, COBRA IIIC, which was developed by Rowe.[3,4] In COBRA IIIC/MIT the same code organization and governing equations were used; however modifications were included which allowed the code to solve much larger problems. In one aspect the equations were solved by iteration rather than by a Gaussian elimination scheme which led to increased efficiency. In addition, internal generation of the physical properties of water and steam were included, and several new correlations were introduced.

The subchannel modeling technique used in COBRA IIIC/MIT is based on the control volume approach. The region of interest in the core is divided radially into a number of flow channels with cross-sectional areas defined by lines joining the fuel rod centers. These channels are then segmented axially to establish the control volumes. Within the channels, fluid properties

such as density, pressure, and velocity are considered to vary in the axial direction only and are assumed to be constant within a control volume. Flow parameters such as enthalpy, flow, pressure, and crossflow are defined at control volume interfaces.

In order to determine the changes in flow conditions between the inlet and outlet of each of the control volumes, it is assumed that variations in the flow parameters are governed by the basic conservation equations for mass, energy, and momentum in both the axial and transverse directions. These governing equations are developed in a finite difference form and solved by a semi-explicit scheme, producing incremental changes in the flow and enthalpy for all control volumes at a given axial height. The procedure is then repeated stepwise up the core using the outlet conditions from the previous step to establish the inlet conditions for the next level of control volumes.

A number of assumptions are made in the development of the model in COBRA IIIC/MIT. First, it is assumed that each subchannel contains a one-dimensional, two-phase, slip flow and that the subchannel density can be determined from flow, enthalpy, pressure, and velocity. A straightforward one-dimensional analysis can then be used within the channels. Secondly, the assumption is made that the subchannels are coupled by both turbulent

and diversion crossflow. However the former does not result in any net flow redistribution. In addition, it is assumed that the sonic velocity propagation of pressure fronts can be ignored, limiting the use of the model to transients with times that are longer than the time for a sonic wave to pass through the subchannel.

2.2 Fluid Transport Model

The fluid transport model used as developed by Rowe[3] in COBRA IIIC/MIT is based on the equations for the mass, energy, and momentum balance in both the axial and transverse direction. The general form of these equations can be constructed by applying the conservation principle to a specific control volume in subchannel i and simplifying the resulting equations by the assumptions previously discussed. For simplicity, lateral interaction is represented as occurring between the volume of interest and only one other adjacent channel j. For the inclusion of all neighboring channels, the coupling terms in the equations may be summed over all of the interconnected subchannels.

The conservation equation

$$A_i \frac{\partial \rho_i}{\partial t} + \frac{\partial m_i}{\partial x} = -w_{ij} \qquad (1)$$

accounts for the net rate of flow change within subchannel i in terms of the diversion crossflow per unit length, w_{ij},

which is considered to be positive when the flow is out of subchannel i, and the time derivative of density which allows for flow changes due to fluid contraction or expansion. Because turbulent crossflow is assumed to cause no net flow change, it is not included in equation (1).

The energy equation used in COBRA IIIC/MIT is

$$\frac{1}{u''}\frac{\partial h_i}{\partial t} + \frac{\partial h_i}{\partial x} = \frac{q_i'}{m} - (h_i - h_j)\frac{w_{ij}'}{m_i} - (T_i - T_j)\frac{c_{ij}}{m_i} + (h_i - h_{ij}^*)\frac{w_{ij}}{m_i} \qquad (2)$$

The terms on the right side of the equation represent the four means by which thermal energy can be transported into a subchannel. The first is the power-to-flow ratio which indicates the change in the enthalpy if thermal mixing is ignored. The second term is the thermal energy transported between adjacent subchannels by turbulent crossflow. The third term in equation (2) is the thermal conduction between adjacent subchannel which is assumed to be proportional to the subchannel temperature difference. The thermal conduction coefficient, c_{ij}, is a function of geometric and fluid parameters. The last term is the thermal energy carried by the diversion crossflow. The variables u'' and h_{ij}^* represent the effective velocity for energy transport and enthalpy carried by the diversion crossflow, respectively.

The first two terms on the left side of the equation for the axial momentum balance

$$\frac{1}{A_i}\frac{\partial m_i}{\partial t} - 2u_i\frac{\partial \rho_i}{\partial t} + \frac{\partial \rho_i}{\partial x} = -\left(\frac{m_i}{A_i}\right)^2\left[\frac{\overline{v}_i f_i \phi_i}{2D_i} + \frac{k_i v_i'}{2\Delta x} + A_i\frac{\partial}{\partial x}\left(\frac{v_i'}{A_i}\right)\right]$$

$$-\rho_i g\cos\theta - \frac{f_t}{A_i}(u_i - u_j)\, w_{ij}' + \frac{1}{A_i}(2u_i - u_{ij}^{*})\, w_{ij} \qquad (3)$$

are the transient components of the axial pressure gradient. The first term is due to the time rate of change in the flow, and the second, in the density. On the right side of equation (3), the first two terms represent the frictional, spatial acceleration, and elevation components of the pressure gradient. The remaining crossflow terms account for changes in the subchannel velocity. The factor f_t is included as a correction factor to modify the turbulent crossflow since the analogy between thermal and momentum transport may not be exact.

Because changes in the flow conditions along the subchannels may produce radial pressure gradients, a transverse momentum equation is required to characterize lateral flow. Its purpose is to couple the subchannels so that the pressure gradient determined from the axial momentum equation can be used as the driving force for the transfer of mass, momentum, and energy between subchannels. This transverse momentum equation may be written as

$$\frac{\partial w_{ij}}{\partial t} + \frac{\partial}{\partial x}\left(u_{ij}^{*} w_{ij}\right) + \left(\frac{s}{\ell}\right) C_{ij} w_{ij} = \left(\frac{s}{\ell}\right)(P_i - P_j) \qquad (4)$$

where C_{ij} is a crossflow resistance function which depends on the magnitude but not the direction of the diversion crossflow. The factor u_{ij}^{*} is the axial velocity and $\left(\frac{s}{\ell}\right)$ accounts for the importance of friction and pressure terms versus inertial terms.

These governing equations represent the fluid transport model in COBRA IIIC/MIT and are used to solve for the flow, enthalpy, pressure, and crossflow in each subchannel as a function of axial position and, in transient problems, as a function of time. However, for any problem consisting of more than a few subchannels, the number of governing equations is large. It is therefore more convenient to use vector notation. By using a rectangular matrix [S], and its transpose, $[S]^T$, which specifies the relationships between subchannels, equations (1) through (4) may be rewritten in a more compact form.

If { } is used to denote a column vector, the mass conservation equation becomes

$$[A]\left\{\frac{\partial \rho}{\partial t}\right\} + \left\{\frac{\partial m}{\partial x}\right\} = -[S]^T \{w\} \qquad (5)$$

The energy equation can be written as

$$\left\{\frac{1}{u^{\prime}}\frac{\partial h}{\partial t}\right\} + \left\{\frac{\partial h}{\partial x}\right\} = \left[\frac{1}{m}\right]\left\{q^{\prime}\right\} - \left[\frac{1}{m}\right][S]^{T}[\Delta h]\{w^{\prime}\}$$

$$-\left[\frac{1}{m}\right][S]^{T}[\Delta T]\{c\} + \left[\frac{1}{m}\right]\left[[h][S]^{T} - [S]^{T}[h^{*}]\right]\{w\} \qquad (6)$$

The axial momentum equation becomes

$$\left[\frac{1}{A}\right]\left\{\frac{\partial m}{\partial t}\right\} - \left\{2u\frac{\partial \rho}{\partial t}\right\} + \left\{\frac{\partial P}{\partial x}\right\} = \{a^{\prime}\} + \left[\frac{1}{A}\right]\left[[2u][S]^{T}[u^{*}]\right]\{w\} \qquad (7)$$

where

$$\{a^{\prime}\} = -\left\{\left(\frac{m}{A}\right)^{2}\left[\frac{vf\phi}{2D} + \frac{kv^{\prime}}{2\Delta x} + A\frac{\partial (v^{\prime}/A)}{\partial x}\right] + \rho g \cos\theta\right\}$$

$$- f_{t}\left[\frac{1}{A}\right][S]^{T}[\Delta u]\{w^{\prime}\}$$

The transverse momentum equation is

$$\left\{\frac{\partial w}{\partial t}\right\} + \left\{\frac{\partial (u^{*}w)}{\partial x}\right\} + \left(\frac{s}{\ell}\right)[c]\{w\} = \left(\frac{s}{\ell}\right)[S]\{P\} \qquad (8)$$

More detailed information on the derivation of these equations can be found in References 3 and 4.

2.3 Fuel Heat Transfer Model

To determine fuel temperatures a fuel heat transfer model which considers radial heat conduction is included in COBRA IIIC/MIT. Using this model, the fuel is divided into N equally spaced radial temperature nodes plus one node for the cladding located at its outer surface. Using a Taylor's

series approximation to the heat transfer conduction equation

$$(\rho c_p)_f \frac{\partial T}{\partial t} = K_f \left(\frac{\partial^2 T}{\partial r^2} + \frac{1}{r} \frac{\partial T}{\partial r} \right) + q''' \tag{9}$$

for each temperature node and the appropriate boundary conditions, N + 1 equations can be developed as shown in Appendix B. From these equations which form a tridiagonal matrix, the temperatures, defined at the control volume center, are obtained by solving the system with a compact Gaussian elimination routine.

In a specific problem, the heat flux from the fuel surface, $q''_{j-\frac{1}{2}}$, which is also defined at the control volume center, can be computed in two ways. If the fuel temperatures are required for the problem, the heat flux is calculated as a function of the temperature difference between the cladding wall and the fluid by

$$q''_{j-\frac{1}{2}} = h'_{j-\frac{1}{2}} \left(T_w - T_b \right)_{j-\frac{1}{2}} \tag{10}$$

where h' is the surface heat transfer coefficient which is determined by a correlation. If the temperature calculations are not performed, an average heat flux is used.

2.4 Method of Solution

In COBRA IIIC/MIT the variations in the flow parameters are assumed to be governed by the conservation equations for

mass, energy, and momentum. To determine the distributions of the flow parameters, these equations must be solved.

Due to the sequential nature of the solution method used in the code, boundary conditions are required. These may include the inlet enthalpy, mass flow, pressure, or crossflow distributions. An option exists in the code to specify any of these distributions as forcing functions but, in general, the values are difficult to obtain. Since the solution method is iterative, approximate values may be used as inlet boundary conditions, such as an average mass flow and zero crossflow. Within several iterations, the code should converge on the correct inlet conditions for the problem.

According to Masterson and Wolf,[5] after the boundary conditions have been specified, the next step in solving equations (5) through (8) is to determine the crossflow interaction between the subchannels at the first axial level above the core inlet. Since the diversion crossflow is assumed to be governed by pressure variations between the flow channels, the pressure field in the region must be determined.

To develop an equation defining the pressure vector for all subchannels at a given axial location, equation (5) for mass conservation and equation (7) for the axial momentum balance are written in a difference form and combined to eliminate the time derivative of the density.

$$[A_j]^{-1}\left\{\frac{m_j - \bar{m}_j}{\Delta t}\right\} + [2u_j][A_j]^{-1}\left\{\frac{m_j - m_{j-1}}{\Delta x}\right\}$$

$$+ [2u_j][A_j]^{-1}[S]^T\{w_j\} + \left\{\frac{P_j - P_{j-1}}{\Delta x}\right\}$$

$$= \{a'_{j-1}\} + [A_j]^{-1}[2u_j][S]^T\{w_j\} - [A_j]^{-1}[S]^T[u_j^*]\{w_j\} \quad (11)$$

Here, the overscore bar (—) indicates a value from a previous time step and the subscripts j and j-1 correspond to axial locations x_j and x_{j-1}. The channel inlet corresponds to j = 1. Because $[A_j]^{-1}$ and $[u_j]$ are diagonal matrices and, as such,

$$[2u_j][A_j]^{-1}[S]^T\{w_j\} = [A_j]^{-1}[2u_j][S]^T\{w_j\} \quad (12)$$

equation (11) can be simplified to

$$[A_j]^{-1}\left\{\frac{m_j - \bar{m}_j}{\Delta t}\right\} + [2u_j][A_j]^{-1}\left\{\frac{m_j - m_{j-1}}{\Delta x}\right\} + \left\{\frac{P_j - P_{j-1}}{\Delta x}\right\}$$

$$= \{a'_{j-1}\} - [A_j]^{-1}[S]^T[u_j^*]\{w_j\} \quad (13)$$

Before this equation can be solved for the pressure distribution, the crossflow term must also be expressed as a function of pressure.

In order to evaluate the crossflow term, the pressure vector {P} and the crossflow resistance terms [C]{w} in

equation (8) are first transformed into the following form:

$$\{P\} = \gamma\{P_j\} + (1-\gamma)\{P_{j-1}\} \tag{14}$$

$$[c]\{w\} = \gamma[c_j]\{w_j\} + (1-\gamma)[c_{j-1}]\{w_{j-1}\} \tag{15}$$

where γ is a weighting function having an arbitrary value between 0.0 and 1.0. By introducing these terms, equation (8) for the transverse momentum balance can be written in a difference form as

$$\left\{\frac{w_j - \bar{w}_j}{\Delta t}\right\} + \left\{\frac{u_j^* w_j - u_{j-1}^* w_{j-1}}{\Delta x}\right\}$$

$$+ \left(\frac{s}{\ell}\right)\left\{\gamma[c_j]\{w_j\} + (1-\gamma)[c_{j-1}]\{w_{j-1}\}\right\}$$

$$= \left(\frac{s}{\ell}\right)[S]\left\{\gamma\{P_j\} + (1-\gamma)\{P_{j-1}\}\right\} \tag{16}$$

The significance of the weighting function can be seen in that it allows the crossflow to be driven by any combination of pressure fields. A value of 0.0 specifies that the crossflow is governed by the pressure field that exists at the bottom of the control volume; a value of 1.0, by the pressure field at the top. Any other value for γ between 0.0 and 1.0 represents a weighted average of the pressures. For a specific problem, it is possible to select an optimum value for the weighting function.

In order to solve equation (16) for the crossflow distribution at successive axial steps, it is rewritten in the form

$$\{w_j\} = [D_j]^{-1}\left\{\left\{\frac{\bar{w}_j}{\Delta t}\right\} + \left\{\frac{u_{j-1}^* w_{j-1}}{\Delta x}\right\} + \left(\frac{s}{\ell}\right)(\gamma-1)[C_{j-1}]\{w_{j-1}\}\right\}$$

$$+ \left(\frac{s}{\ell}\right)[D_j]^{-1}[S]\left\{\gamma\{P_j\} + (1-\gamma)\{P_{j-1}\}\right\} \qquad (17)$$

where

$$[D_j]^{-1} = \left[\frac{1}{\Delta t} + \frac{u_j^*}{\Delta x} + \left(\frac{s}{\ell}\right)\gamma[C_j]\right]^{-1}$$

Now that the crossflow can be expressed as a function of the pressure field, equation (17) is substituted into equation (13), the combined mass-axial momentum equations, and rewritten as

$$\{P_j\} = [I + \gamma M_j]^{-1}[I - (1-\gamma)M_j]\{P_{j-1}\} + [I + \gamma M_j]^{-1}\{b_j\} \qquad (18)$$

where [I] is the identity matrix,

$$[M_j] = \Delta x\left(\frac{s}{\ell}\right)[A_j]^{-1}[S]^T[u_j^*][D_j]^{-1}[S] \quad \text{and}$$

$$\{b_j\} = \Delta x\{a'_{j-1}\} - \left(\frac{\Delta x}{\Delta t}\right)[A_j]^{-1}\{m_j - \bar{m}_j\} - [A_j]^{-1}[2u_j]\{m_j - m_{j-1}\}$$

$$- \Delta x[A_j]^{-1}[S]^T[u_j^*]\ [D_j]^{-1}[S]$$

$$\times\left\{\frac{\bar{w}_j}{\Delta t} + \frac{u_{j-1}^* w_{j-1}}{\Delta x} + \left(\frac{s}{\ell}\right)(\gamma-1)[C_{j-1}]\{w_{j-1}\}\right\}$$

Note that in the first iteration, two of the vectors required to compute $\{b_j\}$ are unknown: $\{m_j\}$, the mass flow, and $\{w_j\}$, the diversion crossflow. However, by assuming this initial crossflow to be zero and by estimating the mass flow by an averaged value, an approximate pressure field can be calculated using equation (18), when an inlet pressure boundary condition is used to specify the vector $\{P_{j-1}\}$.

With the initial pressure distribution determined by equation (18), the crossflow distribution can be obtained by solving equation (17). Once the crossflows have been established, the mass flow can be computed using the mass conservation equation in the form of

$$m_j = \Delta x\left\{[S]^T\{w_j\} - [A_j]\left\{\frac{\rho_j - \bar{\rho}_j}{\Delta t}\right\} + \frac{m_{j-1}}{\Delta x}\right\}$$

With the calculation of the mass flow at position j, the first iteration for the initial set of control volumes is completed. The second and successive iteration follow a slightly different scheme which takes advantage of the most recently calculated values. A new pressure field, $\{P_j'\}$ is generated by the difference form of the axial momentum equation

$$[A_j]^{-1}\left\{\frac{m_j - \bar{m}_j}{\Delta t}\right\} - [2u_j]\left\{\frac{\rho_j - \bar{\rho}_j}{\Delta t}\right\} + \left\{\frac{P_j - P_{j-1}}{\Delta x}\right\}$$

$$= \{a'_{j-1}\} + [A_j]^{-1}\left[[2u_j][S]^T - [S]^T[u_j^*]\right]\{w_j\} \qquad (20)$$

and using the previously computed values for the axial mass flow distribution, $\{m_j\}$, and the crossflow distribution, $\{w_j\}$. This new pressure distribution is averaged with the pressure field at the bottom of the control volume $\{P_{j-1}\}$ using the weighted function shown in equation (14). The resulting composite pressure distribution is used to solve for the crossflows by equation (17), which are then used to compute the new axial mass flow distribution by equation (19). This iteration procedure continues until the mass flow changes fall below a chosen convergence criterion. When convergence is achieved, the process is allowed to sweep downstream to the next axial level at which the previously calculated pressure, crossflow, and mass flow distributions are now used as inlet conditions for the next set of control volumes.

The energy balance is performed using the converged solution to the axial momentum equation for the mass flow, $\{m_j\}$. This is accomplished by solving the difference form of the energy equation, equation (6),

$$\left\{\frac{1}{u''}\right\}\left\{\frac{h_j - \bar{h}_j}{\Delta t}\right\} + \left\{\frac{h_j - h_{j-1}}{\Delta x}\right\} = \{m_j\}^{-1}\left\{\{q''_{j-\frac{1}{2}}\}\right.$$

$$\left. - [S][\Delta h_{j-1}]\{w'_{j-1}\} - [S]^T[\Delta t_{j-1}][c_{j-1}]\right\}$$

$$+ \{m_j\}^{-1}\left[[h_{j-1}][S]^T - [S]^T[h^*_{j-1}]\right] \qquad (21)$$

for the enthalpy of the fluid at a new axial level, $\{h_j\}$. The enthalpy value at the previous level, $\{h_{j-1}\}$, and the heat flux determined by the fuel heat transfer model are used.

Once all of the flow conditions have been determined, the critical heat flux at which DNB occurs can be calculated from a correlation. From this and the heat flux previously calculated, the DNBR can be determined.

For a transient problem, a time loop is used to continue the numerical scheme through successive time steps of Δt. At the beginning of each time step, the boundary conditions are set as required by the problem and the steady-state solution procedure is repeated as described above until the flow field converges. This scheme is followed until the end of the transient is reached.

III. COBRA IIIC/MIT INPUT DATA

3.1 Reactor Core Description

In this analysis the model of the reactor core is based on the Trojan Nuclear Power Plant operated by Portland General Electric Company. It is a Westinghouse pressurized water reactor with a thermal rating of 3411 MW. The active core region is an approximate right circular cylinder with an equivalent diameter of 132.7 inches (337.1 cm) and an active height of 143.7 inches (365.0 cm). The core is composed of an array of fuel assemblies which are square in cross-section, measuring 8.426 inches (21.4 cm) on a side. The fuel rods in the assembly are arranged in a square array with 17 positions per side and consist of uranium dioxide pellets encased in a Zircaloy-4 cladding. Of the possible 289 locations per assembly, 24 are occupied by guide thimbles and one is used for in-core instrumentation.

In addition to the fuel rods and guide thimbles, an assembly consists of a top nozzle, a bottom nozzle, and eight grid spacer assemblies. The basic support for the fuel rods in the assembly is supplied by these grid spacers, which are fastened to the guide thimbles at locations along the height of the fuel where lateral support is required, and by the top and bottom nozzle.

Information required by COBRA IIIC/MIT to model the core, including nominal operating conditions and core design parameters, is given on Tables 1 and 2 and was obtained from the Trojan Final Safety Analysis Report (FSAR).[6]

3.2 Thermal Hydraulic Input

COBRA IIIC/MIT was developed to analyze a wide variety of problems. Since these problems may be described by a broad range of conditions, not all thermal hydraulic parameters may apply. They are therefore designed to be introduced to the code as input parameters. These thermal hydraulic parameters as used in the present analysis are shown in Table 3.

Various correlations are also required in the code to model the thermal hydraulic behavior of the reactor core. A number of built-in correlations have been included in COBRA IIIC/MIT. The code requires specification of the correlations and the input coefficients applicable to the problem. Table 4 lists those chosen for this analysis. The critical heat flux and subcooled void correlations are not shown due to their complexity but are described in References 7 and 8.

In addition to the parameters and the correlations, data concerning the grid spacer assemblies is required.

Table 1

NOMINAL OPERATING CONDITIONS AND THERMAL DATA

Core Power, MW_t	3411
System Pressure, psia	2250
Coolant Inlet Temperature, °F	552.5
Coolant Flow	
Effective Flow Area, ft^2	51.1
Core Flow Rate, lb/hr	132.7×10^6
Average Mass Velocity, lb/hr-ft^2	2.48×10^6
Heat Transfer	
Fraction of Heat Generated in Fuel, %	97.4
Total Core Heat Transfer Area, ft^2	59,700
Average Heat Flux, Btu/hr-ft^2	1.898×10^5
Average Linear Power, kW/ft	5.44

Table 2

CORE DESIGN PARAMETERS

Fuel Assembly	
Number per Core	193
Rod Array	17 x 17
UO_2 Rods per Assembly	264
Rod Pitch, in.	0.496
Overall Dimension, in.	8.426 x 8.426
Number Grids per Assembly	8
Fuel Rod	
Number per Core	50,952
Outside Diameter, in.	0.374
Diameter Gap, in.	.0065
Clad Thickness, in.	.0225
Clad Material	Zircaloy-4
Fuel Pellet	
Diameter, in.	.3225
Material	UO_2 Sintered
Guide Thimble	
Outside Diameter, in.	.482

Table 3

THERMAL HYDRAULIC PARAMETERS

Diversion Crossflow Resistance Factor	0.5
Turbulent Momentum Factor	0.0
Transverse Momentum Factor	0.25
Thermal Diffusion Coefficient	0.038
Flow Convergence	0.01

Table 4

THERMAL HYDRAULIC CORRELATIONS

Critical Heat Flux:	Westinghouse W-3 Correlation[7]
Heat Transfer Coefficient:	Thom Two Phase Model
Single Phase--	$h' = 0.134\ (K/D)\ Re^{0.65}\ Pr^{0.4}$
	$T_w = T_b + q''/h'$
Subcooled Boiling--	$T_w = T_{sat} + 0.072\ q''^{0.5}/e^{P/1260}$
	$h' = (T_w - T_b)/q''$
Subcooled Voids:	Levy Model[8]
Void Fraction:	Homogeneous Model
$\alpha = 0.$	for $X \leq 0.$
$\alpha = \frac{Xv_g}{(1-X)v_f + Xv_g}$	for $X > 0.$
Two Phase Friction Multiplier:	Homogeneous Model
$\phi = 1.0$	for $X \leq 0.$
$\phi = \frac{\rho_f}{\rho}$	for $X > 0.$
Single Phase Friction Factor:	$0.184\ Re^{-0.2}$
(wall viscosity correction to the friction factor is included)	
Subcooled Turbulent Mixing:	$0.0062\ Re^{-0.1}$

The locations of the grid spacers and the associated loss coefficients as used in this analysis are shown in Table 5. The loss coefficient at the top of the fuel assembly accounts for pressure drop through the nozzle as well as the grid spacer assembly.

An axial heat flux is also required to calculate the DNBR. Since this distribution can change as a result of variations in the control rod locations, power level, or xenon transients, a number of profiles may be specified. The particular axial heat flux chosen for this study is given as the reference DNB design axial shape used in the Trojan FSAR. This distribution is a chopped cosine shape with a peak average value of 1.55. Table 6 shows the axial locations and relative heat flux used as input for the code to represent this design axial shape.

3.3 Reactor Core Modeling

A subchannel layout must be set up in COBRA IIIC/MIT in order for the code to evaluate the flow and enthalpy in the core. Since computer storage capacity is limited and running time should be optimized to save cost, it is not possible to include every subchannel and fuel rod in the core. It is therefore necessary to reduce the model to a reasonable number of pseudo-flow channels which will still enable the code to make an accurate prediction of the DNBR.

Table 5

GRID SPACER ASSEMBLY DATA

Spacer Number	Position x/L	Loss Coefficient
1	.001	3.10
2	.009	1.65
3	.179	1.65
4	.322	1.65
5	.464	1.65
6	.608	1.65
7	.751	1.65
8	.894	1.65
9	.999	4.75

p.29 missing from original. Author unavailable to supply.

Two possibilities can be utilized in modeling the reactor core and still maintaining a reasonable number of channels. First, since the core of a PWR usually exhibits one-eighth core symmetry it is possible to use a one-eighth core model. Secondly, in regions of little significance for DNBR calculations such as at the core periphery, the subchannels and fuel rods can be lumped together into a larger unit. In regions of high interest such as in and near the hot channel, the individual subchannels can be maintained. Thus by making use of the PWR core property of symmetry and by using channel lumping, it is possible to retain as many subchannels as are required for hot channel detail while allowing an adequate representation of the remainder of the core.

Figure 1 shows the assembly radial power distribution and core layout selected for this DNBR analysis. Due to the effects of fuel depletion and changes in control rod positions and spatial xenon distribution during the normal operation of a reactor, a number of power distributions can be specified. This particular reference case is representative of an unrodded core at hot zero power near the beginning of life. The location of the hot assembly for this power distribution is shown in Figure 1.

Using the core layout shown in Figure 1, a one-eighth core model can be designed as shown in Figure 2.

Figure 1

Assembly Radial Power Distribution and Core Layout

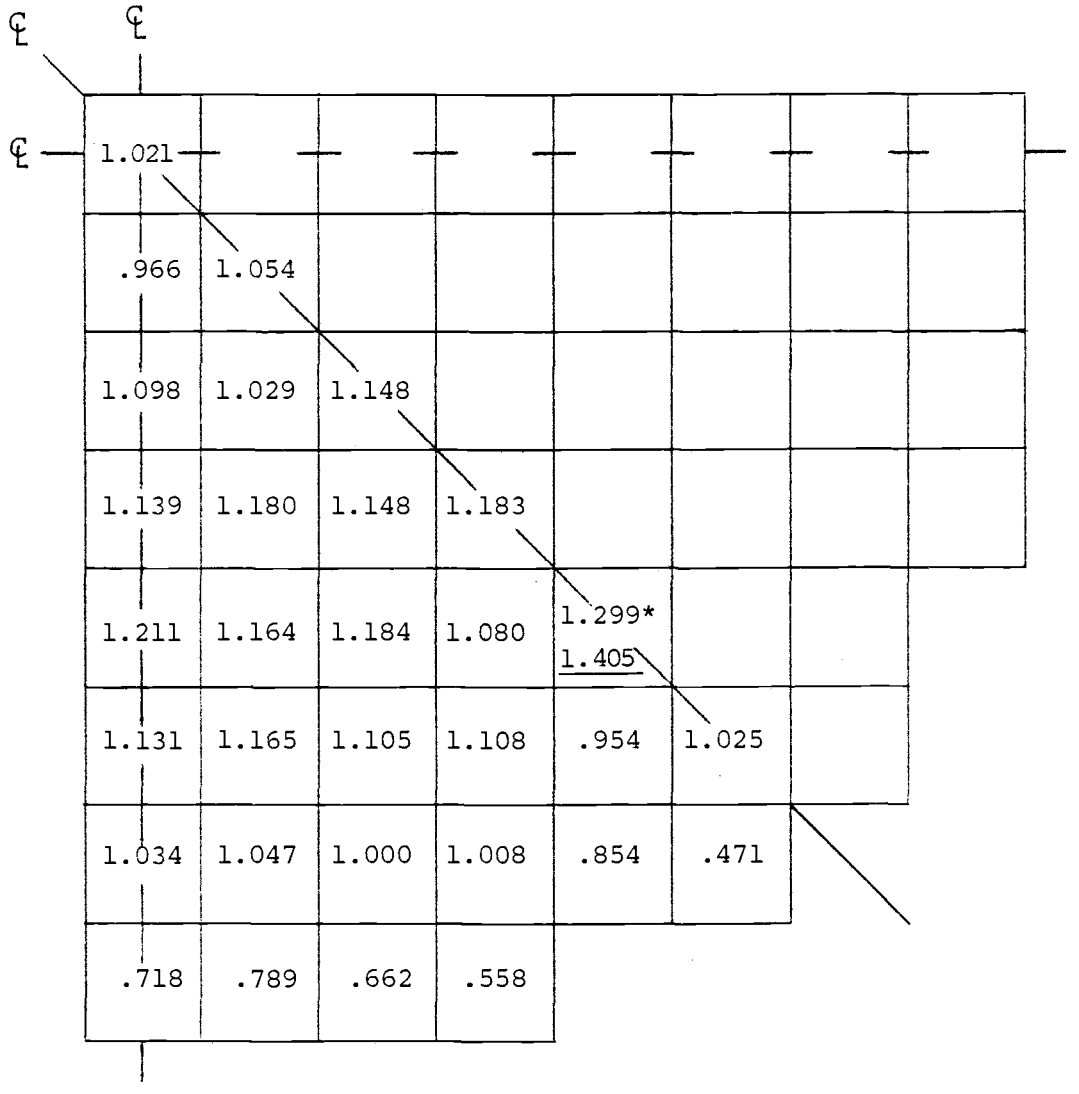

X.XXX Radial Power Factor

X.XXX Maximum Assembly Power

* Location of hot assembly

Figure 2

Model for Core-Wide DNBR Analysis

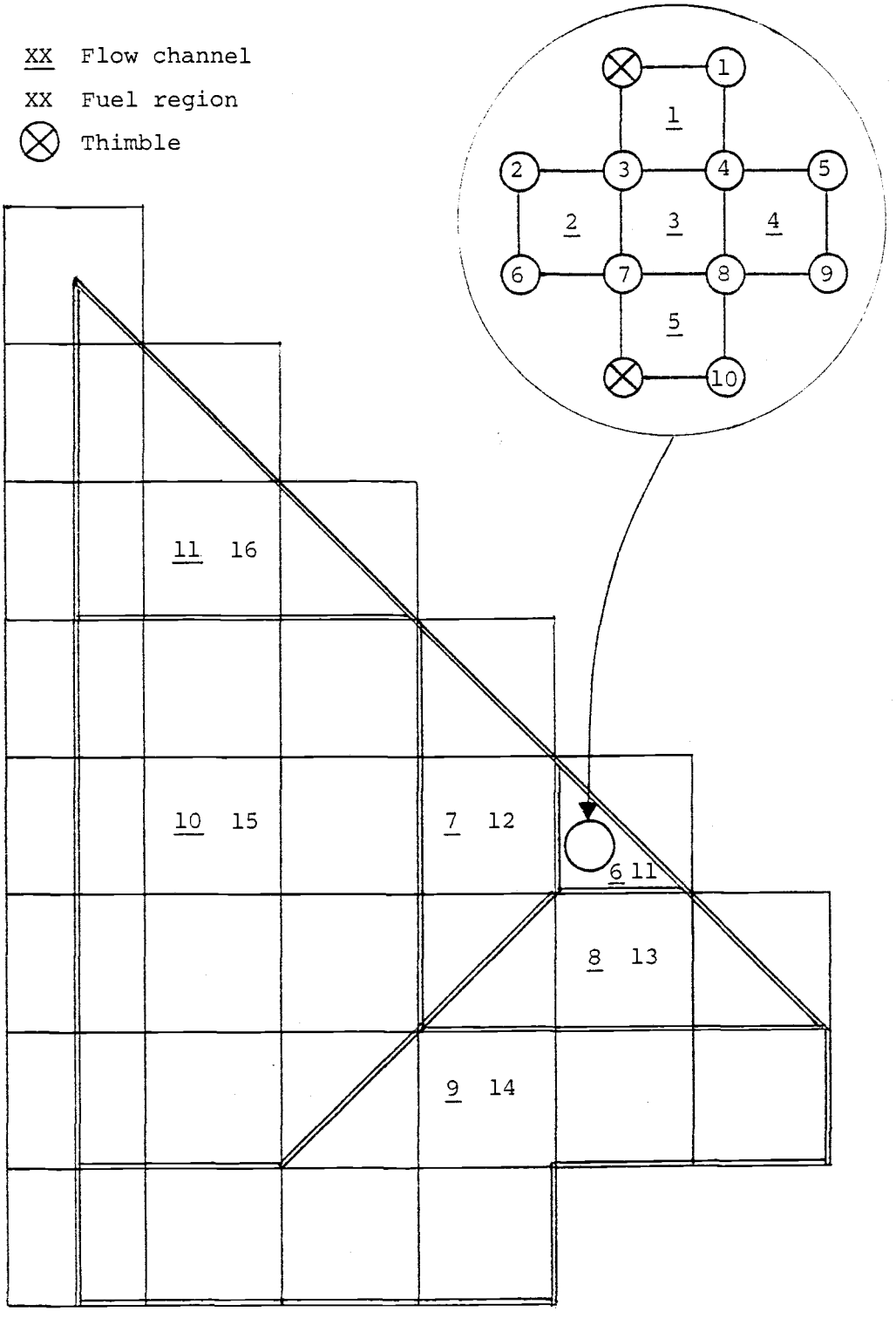

It incorporates fine detail in and around the hot channel, yet lumps the remaining flow and fuel regions in order to reduce the size of the problem. Tables 7 and 8, respectively, show the fuel region and channel parameters calculated from this model which are used for the DNBR analysis.

In Table 7, the fraction of power to the adjacent channels was calculated by a method described by Ladieu[9] which is given in Appendix C. It includes allowances for the engineering hot channel factors and the fraction of heat which is generated in the fuel. For fuel regions 11 through 16, the large fraction of power to adjacent channels is due to the greater number of fuel rods actually located in the regions. The channel flow areas shown in Table 8 for regions 6 through 11 also show the effect of lumping. The spacing for crossflow to adjacent channels listed represents the gap between the fuel rods at a region boundary which creates the area available for crossflow.

The radial power factors for the lumped fuel regions are weighted averages obtained from the assembly radial power distribution shown in Figure 1. Because the position of the hot channel varies due to local conditions, a reference design was chosen for the radial power factors within the hot assembly in which detail rods are assumed to be at peak power while all remaining lumped rods are at the assembly average.

Table 7

FUEL REGION PARAMETERS FOR DNBR ANALYSIS

Rod No.	Diameter (in.)	Radial Power Factor	Fraction of Power to Adjacent Channels (Adj. Channel No.)			
1	0.3740	1.4050	0.2492 (1)	0.7476 (6)		
2	0.3740	1.4050	0.2492 (2)	0.7476 (6)		
3	0.3740	1.4050	0.2492 (1)	0.2492 (2)	0.2666 (3)	0.2492 (6)
4	0.3740	1.4050	0.2492 (1)	0.2666 (3)	0.2492 (4)	0.2492 (6)
5	0.3740	1.4050	0.2492 (4)	0.7476 (6)		
6	0.3740	1.4050	0.2492 (2)	0.7476 (6)		
7	0.3740	1.4050	0.2492 (2)	0.2666 (3)	0.2492 (5)	0.2492 (6)
8	0.3740	1.4050	0.2666 (3)	0.2492 (4)	0.2492 (5)	0.2492 (6)
9	0.3740	1.4050	0.2492 (4)	0.7476 (6)		
10	0.3740	1.4050	0.2492 (5)	0.7476 (6)		
11	0.3740	1.2990	125.3 (6)			
12	0.3740	1.1130	542.1 (7)			
13	0.3740	1.0100	542.1 (8)			
14	0.3740	0.7430	1897.0 (9)			
15	0.3740	1.1320	2575.0 (10)			
16	0.3740	1.0530	847.0 (11)			

Table 8

CHANNEL PARAMETERS FOR DNBR ANALYSIS

Channel No.	Area (Sq.-In.)	Wetted Perim. (In.)	Heated Perim. (In.)	Adjacent Channel No., Spacing for Crossflow	
1	0.1180	1.260	0.8812	3, 0.122	6, 0.258
2	0.1362	1.175	1.1750	3, 0.122	6, 0.366
3	0.1362	1.175	1.1750	4, 0.122	5, 0.122
4	0.1362	1.175	1.1750	6, 0.366	
5	0.1180	1.260	0.8812	6, 0.258	
6	18.07	168.0	149.8	7, 2.068	8, 2.068
7	74.87	696.1	620.4	8, 5.018	10, 6.204
8	74.87	696.1	620.4	9, 6.204	
9	262.0	2436.	2171.	10, 8.120	
10	355.6	3306.	2947.	11, 5.170	
11	117.0	1088.	969.3		

IV. SENSITIVITY ANALYSIS

The DNBR is a function of a number of variables and can be calculated using COBRA IIIC/MIT. Before developing a response surface which represents the functional relationship between the input variables and the resulting DNBR, it is necessary to consider whether all input variables should play an equal part in the construction of the approximate function to represent the computer code. In order to determine the variables which are significant and must be retained for the subsequent analysis, a sensitivity analysis was performed.

The input variables used for this analysis are shown on Table 9. Also included are the nominal values for each variable and the magnitude of its uncertainty assumed for a level of two standard deviations. These measurements of uncertainty are established through engineering judgment and are chosen to be representative. Variations in the thermal hydraulic parameters and correlations are not considered. Although the accuracy of these parameters and correlations is not known exactly, their effect is believed to be small. Sensitivity studies by Rowe[3] indicate only a minimal effect on the thermal performance due to the variations in the thermal hydraulic parameters.

The first four parameters on Table 9, including the system pressure, inlet temperature of the coolant,

Table 9

VALUES OF INPUT PARAMETERS FOR SENSITIVITY ANALYSIS

Parameter	Nominal Value	2σ Uncertainty (%)
1) Reactor System Pressure, psia	2250	2
2) Coolant Inlet Temperature, °F	552.5	1
3) Average Mass Velocity, lb/hr-ft^2	2.48×10^6	6
4) Average Heat Flux, Btu/hr-ft^2	1.898×10^5	2
5) Gap Coefficient, Btu/hr-ft^2-°F	1000.	30
6) Fuel Density, lb/ft^3	650.	10
7) Clad Density, lb/ft^3	500.	10
8) Fuel Heat Capacity, Btu/lb-°F	0.085	10
9) Clad Heat Capacity, Btu/lb-°F	0.09	10
10) Fuel Heat Conductivity, Btu/hr-°F-ft	1.5	10
11) Clad Heat Conductivity, Btu/hr-°F-ft	12.0	10
12) Grid Spacer Loss Coefficients		
Type 1	3.1	10
Type 2	1.65	
Type 3	4.75	

and average mass velocity and heat flux have been shown to directly affect the value of the DNBR in previous work done by Chunis.[10] Parameters 5 through 11 do not affect DNBR directly but are used in the code to calculate the fuel temperature distribution, the results of which are used to determine the local heat flux for the DNBR. These seven parameters are included in the sensitivity analysis because, though utilized in COBRA IIIC/MIT as constants, they are functions of temperature. The effect of using these input parameters as constants may contribute to the overall error in the analysis, so that it is important to determine the significance of each parameter. The last parameter listed on Table 9 is the grid spacer loss coefficients which are used to calculate the pressure drop along the subchannel due to flow through the spacer assemblies. Though the coefficients have been shown to be functions of coolant flow conditions,[11] they too are treated as constants within the code.

The sensitivity analysis begins by varying each parameter over a range of values while all others are held fixed at the nominal values. A total of five values is used for each input variable including its nominal value, μ, and the four values $\mu \pm 2\sigma$ and $\mu \pm 4\sigma$ where σ is the standard deviation specified on Table 9.

Over the range of five points used in this initial analysis, the last eight input parameters, including the fuel and clad physical properties and the grid spacer loss coefficients, showed no effect upon the calculated DNBR. Because of this apparent insensitivity, they were eliminated from the subsequent analysis and were used only at the chosen nominal values. From these results, it appears that the use of these parameters as constants has no effect upon the DNBR calculation for this steady-state analysis.

Figure 3 shows the results of the analysis for the first four parameters. For each, a profile based on the five points has been plotted to represent the effect of the variable on the DNBR when all other variables are held fixed at the nominal values. Notice that the horizontal scale is generalized in terms of standard deviation such that

$$y_i' = \frac{y_i - \mu_i}{2\sigma_i}$$

where y_i' is the transformed variable corresponding to the original y_i. Because the values of the standard deviations vary, the actual scale depends on the input parameter to which it refers.

Figure 3

Changes in DNBR Due to Variations in Input Parameters 1 - 4

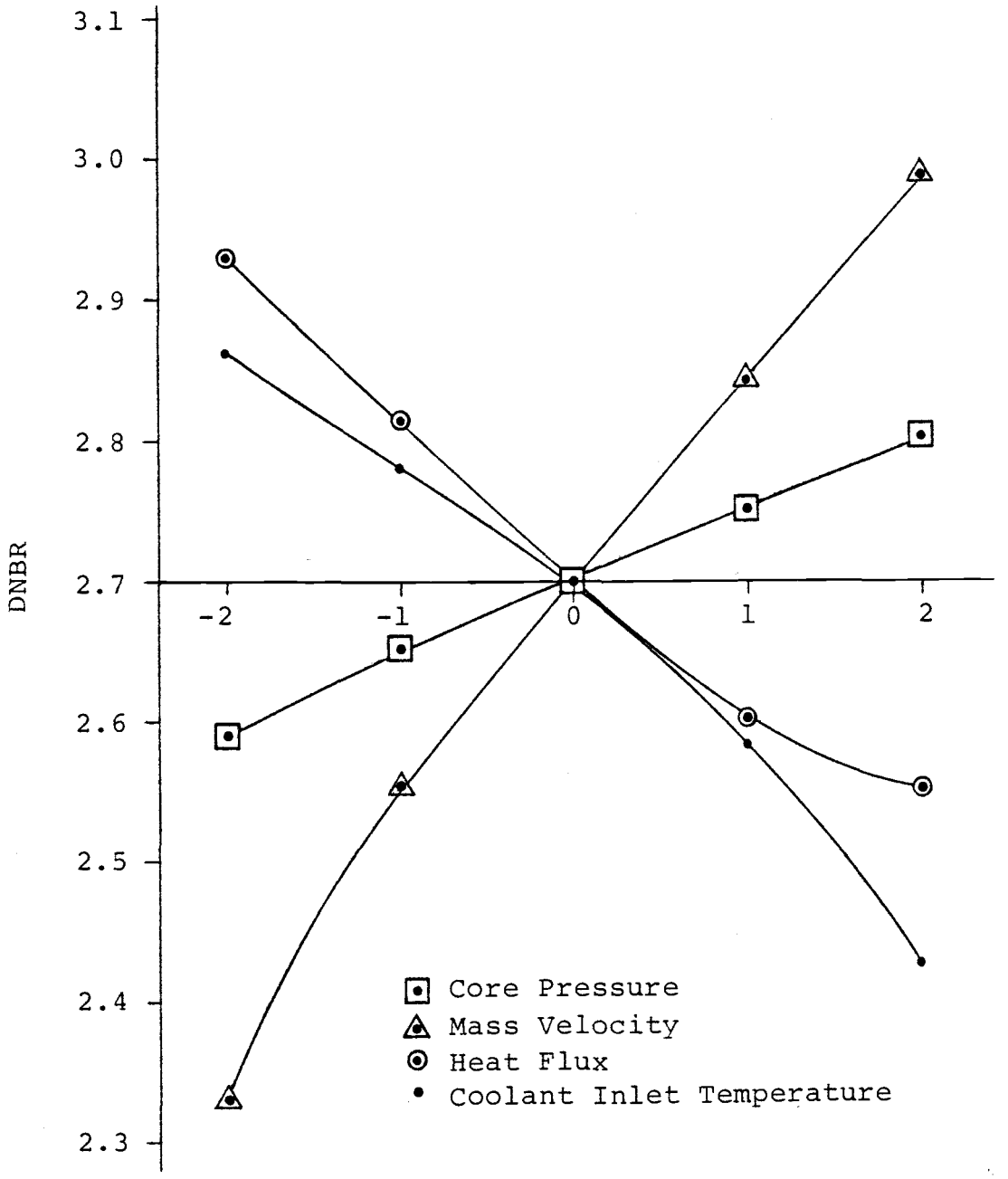

This method allows a visual appreciation of the form of the response and also serves to indicate if variable transformation is required on significant variables, assuming only a second-order polynomial is to be used to fit the response surface.

The results obtained indicate that the DNBR is most sensitive to coolant mass velocity; as it increases, so does the DNBR. The DNBR is also shown to be directly related to the core pressure but is inversely related to the coolant inlet temperature and average heat flux. Though the individual responses in Figure 3 are non-linear, the need for variable transformation is not indicated by the profiles.

On the basis of the sensitivity analysis for the twelve input parameters, the DNBR calculation appears to be relatively insensitive to variations in eight of the input parameters. These eight parameters can be eliminated from the subsequent response surface analysis. The remaining four variables, core pressure, coolant inlet temperature, average mass velocity and heat flux, do have a significant effect upon the DNBR and are retained for the development of the response surface.

V. RESPONSE SURFACE DEVELOPMENT

5.1 Background

A computer code such as COBRA represents some functional relationship between the calculated DNBR and the input variables. Over the range of the input, this relationship defines a multi-dimensional surface. Because this surface is obtainable only by extensive use of the code, the complete or true surface cannot be determined easily. Instead, an approximate surface can be developed from the systematic sampling of the true response surface in the form of a polynomial equation including the independent input variables as terms. This polynomial approximation to the true response surface can then be used to examine the behavior of the true surface without the extra cost of repeated runs of the computer code.

The method of sampling the true response surface is controlled by the experimental design. This establishes how best to locate the points at which the computer code is run in order to obtain the maximum statistical information from the fewest possible runs. In general, this statistical information consists of obtaining estimates of the coefficients of the polynomial equation used to approximate the true response surface.

One of the more commonly used experimental designs is the two level factorial design[12] in which each variable or factor is evaluated at two different levels or values. As the name factorial implies, the input variables are perturbed simultaneously over the two chosen levels rather than one-by-one. This approach is useful in assessing the combined effects of two or more factors so that the interaction among variables can be measured. To complete a factorial design consisting of two levels, the required number of computer runs would be 2^k where k is the number of input variables of interest.

A two level factorial design is adequate to estimate the linear and second order interaction coefficients, but not quadratic terms. In order to estimate surface curvature, additional runs are required in which each variable is altered in a one-at-a-time design. The quadratic terms may then be estimated from the base factorial cases plus these additional runs.

Once the sampling of the true response surface is completed as required by the chosen experimental design, the approximating surface function can be generated using a simplified multiple regression routine. At this point, an analysis of variance can be performed in order to develop an adequate model to represent the true response surface in the subsequent evaluations.

5.2 Experimental Design

Experimental designs for fitting a second order response surface must involve at least three levels of each variable. As a factorial design, this would represent 3^k evaluations.

An alternate class of designs, called composite designs, can also be applied to second order response surfaces. The composite designs are first factorial designs that are augmented by a number of additional points which allow the coefficients of the second order surface to be approximated. Fewer computer runs are generally required for the composite designs.

For this analysis, the central composite design[13] was selected. It consists of a 2^k factorial design plus a center point at which all variables are at their nominal values and $2k$ axial points at which the input variables are perturbed one at a time. Considering the four input variables identified in the sensitivity analysis, this represents a total of 25 evaluations of the DNBR using the computer code. Table 10 lists the design matrix, [D], and the corresponding DNBR evaluations, {y}. The input variables for reactor system pressure, (P), coolant inlet temperature, (T), average mass velocity, (G), and average heat flux, (Q), are variables x_1, x_2, x_3, and x_4, respectively. The matrix

Table 10

DESIGN MATRIX AND CORRESPONDING DNBR

$$[D] = \begin{bmatrix} x_1 & x_2 & x_3 & x_4 \\ -1 & -1 & -1 & -1 \\ 1 & -1 & -1 & -1 \\ -1 & 1 & -1 & -1 \\ 1 & 1 & -1 & -1 \\ -1 & -1 & 1 & -1 \\ 1 & -1 & 1 & -1 \\ -1 & 1 & 1 & -1 \\ 1 & 1 & 1 & -1 \\ -1 & -1 & -1 & 1 \\ 1 & -1 & -1 & 1 \\ -1 & 1 & -1 & 1 \\ 1 & 1 & -1 & 1 \\ -1 & -1 & 1 & 1 \\ 1 & -1 & 1 & 1 \\ -1 & 1 & 1 & 1 \\ 1 & 1 & 1 & 1 \\ -1.414 & 0 & 0 & 0 \\ 1.414 & 0 & 0 & 0 \\ 0 & -1.414 & 0 & 0 \\ 0 & 1.414 & 0 & 0 \\ 0 & 0 & -1.414 & 0 \\ 0 & 0 & 1.414 & 0 \\ 0 & 0 & 0 & -1.414 \\ 0 & 0 & 0 & 1.414 \\ 0 & 0 & 0 & 0 \end{bmatrix} \qquad \{y\} = \begin{bmatrix} \\ 2.701 \\ 2.793 \\ 2.438 \\ 2.565 \\ 2.992 \\ 3.111 \\ 2.753 \\ 2.858 \\ 2.542 \\ 2.639 \\ 2.284 \\ 2.376 \\ 2.830 \\ 2.941 \\ 2.527 \\ 2.707 \\ 2.629 \\ 2.771 \\ 2.818 \\ 2.528 \\ 2.475 \\ 2.904 \\ 2.863 \\ 2.576 \\ 2.706 \end{bmatrix}$$

elements represent coded values corresponding to the transformation used in the sensitivity analysis (equation 22). The measured level for the variables associated with each of the five coded levels used in the experimental design are given in Table 11.

5.3 Response Surface Fitting

Using the data obtained at the experimental design points, a second-degree polynomial must now be fit. For the second order response model

$$\hat{y} = b_0 + \sum_{i=1}^{4} b_i x_i + \sum_{i=1}^{4} b_{ii} x_i^2 + \sum_{\substack{i \\ i<j}} \sum_{j} b_{ij} x_i x_j \qquad (23)$$

where $\hat{y}$ represents the estimated response, the coefficient estimation matrix, $[x]$, is shown in Table 12. The equations representing the system can then be written in vector notation as

$$[x]\{b\} = \{\hat{y}\} \qquad (24)$$

where $\{b\}$ represents the polynomial coefficients vector.

A technique for estimating these coefficients is the method of least squares[14] for which the normal equations may be written as

$$[x]^T[x]\{b\} = [x]^T\{y\} \qquad (25)$$

The column vector, $\{b\}$, can then be defined by multiplying

Table 11

MEASURED AND CODED FACTOR LEVELS

		-1.414	-1.000	0.000	1.000	1.414
x_1	System Pressure, psia	2186.	2205.	2250.	2295.	2314.
x_2	Coolant Inlet Temp., °F	544.7	547.0	552.5	558.0	560.3
x_3	Average Mass Velocity, 10^6 lb/hr-ft^2	2.270	2.331	2.480	2.629	2.690
x_4	Average Heat Flux, 10^5 Btu/hr-ft^2	1.844	1.860	1.898	1.936	1.952

Table 12

COEFFICIENT ESTIMATION MATRIX

$$[x] = \left[\begin{array}{c|c|cccccccccc} & x_1\ x_2\ x_3\ x_4 & x_1^2 & x_2^2 & x_3^2 & x_4^2 & x_1x_2 & x_1x_3 & x_1x_4 & x_2x_3 & x_2x_4 & x_3x_4 \\ \hline 1 & & 1 & 1 & 1 & 1 & 1 & 1 & 1 & 1 & 1 & 1 \\ 1 & & 1 & 1 & 1 & 1 & -1 & -1 & -1 & 1 & 1 & 1 \\ 1 & & 1 & 1 & 1 & 1 & -1 & 1 & 1 & -1 & -1 & 1 \\ 1 & & 1 & 1 & 1 & 1 & 1 & -1 & -1 & -1 & -1 & 1 \\ 1 & & 1 & 1 & 1 & 1 & 1 & -1 & 1 & -1 & 1 & -1 \\ 1 & & 1 & 1 & 1 & 1 & -1 & 1 & -1 & -1 & 1 & -1 \\ 1 & & 1 & 1 & 1 & 1 & -1 & -1 & 1 & 1 & -1 & -1 \\ 1 & & 1 & 1 & 1 & 1 & 1 & 1 & -1 & 1 & -1 & -1 \\ 1 & & 1 & 1 & 1 & 1 & 1 & 1 & -1 & 1 & -1 & -1 \\ 1 & & 1 & 1 & 1 & 1 & -1 & -1 & 1 & 1 & -1 & -1 \\ 1 & & 1 & 1 & 1 & 1 & -1 & 1 & -1 & -1 & 1 & -1 \\ 1 & [D] & 1 & 1 & 1 & 1 & 1 & -1 & 1 & -1 & 1 & -1 \\ 1 & & 1 & 1 & 1 & 1 & 1 & -1 & -1 & -1 & -1 & 1 \\ 1 & & 1 & 1 & 1 & 1 & -1 & 1 & 1 & -1 & -1 & 1 \\ 1 & & 1 & 1 & 1 & 1 & -1 & -1 & -1 & 1 & 1 & 1 \\ 1 & & 1 & 1 & 1 & 1 & 1 & 1 & 1 & 1 & 1 & 1 \\ 1 & & 2 & 0 & 0 & 0 & 0 & 0 & 0 & 0 & 0 & 0 \\ 1 & & 2 & 0 & 0 & 0 & 0 & 0 & 0 & 0 & 0 & 0 \\ 1 & & 0 & 2 & 0 & 0 & 0 & 0 & 0 & 0 & 0 & 0 \\ 1 & & 0 & 2 & 0 & 0 & 0 & 0 & 0 & 0 & 0 & 0 \\ 1 & & 0 & 0 & 2 & 0 & 0 & 0 & 0 & 0 & 0 & 0 \\ 1 & & 0 & 0 & 2 & 0 & 0 & 0 & 0 & 0 & 0 & 0 \\ 1 & & 0 & 0 & 0 & 2 & 0 & 0 & 0 & 0 & 0 & 0 \\ 1 & & 0 & 0 & 0 & 2 & 0 & 0 & 0 & 0 & 0 & 0 \\ 1 & & 0 & 0 & 0 & 0 & 0 & 0 & 0 & 0 & 0 & 0 \end{array}\right]$$

each side of equation (25) by the inverse of $[x]^T[x]$.

$$\{b\} = ([x]^T[x])^{-1}\,[x]^T\{y\} \qquad (26)$$

The second order response surface developed by this method is given in Table 13. The polynomial is listed in a vertical format so that the DNBR is the sum of terms consisting of the product of each variable and its coefficient. The coefficients of multiple determination, denoted by R^2, for the full model is 0.9951. (When all observations correspond directly to the fitted response surface, R^2 takes on the value of 1.)

An analysis of variance can be conducted at this point to test for the significance of regression due to the full model variables. Table 14 summarizes the results. Due to the use of a computer code to evaluate the DNBR, the analysis includes no experimental error. Hence, the error term in the analysis of variance table represents lack-of-fit for the data, not error due to the random variation between observations under the same conditions.

An F-statistic, the ratio of the regression variable mean square to mean square error, can be used to test for the significance of the variable in accounting for model-data variation. Using a significance level of 0.10, nine out of the fourteen total terms can be eliminated.

Table 13

FULL MODEL RESPONSE SURFACE

Coefficient	Variable
2.7021	1
5.6191×10^{-2}	x_1
-1.2256×10^{-1}	x_2
1.4939×10^{-1}	x_3
-8.8544×10^{-2}	x_2
-5.7492×10^{-4}	x_1
-1.4075×10^{-2}	x_2^2
-5.8250×10^{-3}	x_3^2
9.1753×10^{-3}	x_4^2
5.3125×10^{-3}	x_1x_2
6.6875×10^{-3}	x_1x_3
2.3125×10^{-3}	x_1x_4
-1.0625×10^{-3}	x_2x_3
-4.6875×10^{-3}	x_2x_4
-3.3125×10^{-3}	x_3x_4

$R^2 = 0.9951$

Table 14

ANALYSIS OF VARIANCE

Source of Vatiation	Sum of Squares	Degrees of Freedom	Mean Square	F
Regression				
Linear	9.667×10^{-1}	4	2.417×10^{-1}	
x_1	6.315×10^{-2}	1	6.315×10^{-2}	132.34*
x_2	3.004×10^{-1}	1	3.004×10^{-1}	629.55*
x_3	4.463×10^{-1}	1	4.463×10^{-1}	995.35*
x_4	1.568×10^{-1}	1	1.568×10^{-1}	328.61*
Quadratic	2.532×10^{-3}	4	6.331×10^{-4}	
x_1^2	2.645×10^{-6}	1	2.645×10^{-6}	.005
x_2^2	1.584×10^{-3}	1	1.584×10^{-3}	3.32*
x_3^2	2.714×10^{-4}	1	2.714×10^{-4}	.57
x_4^2	6.734×10^{-4}	1	6.734×10^{-4}	1.411
Interaction	1.798×10^{-3}	6	2.996×10^{-4}	
x_1x_2	4.516×10^{-4}	1	4.516×10^{-4}	.95
x_1x_3	7.156×10^{-4}	1	7.156×10^{-4}	1.50
x_1x_4	8.556×10^{-5}	1	8.556×10^{-5}	.18
x_2x_3	1.806×10^{-5}	1	1.806×10^{-5}	.04
x_2x_4	3.516×10^{-4}	1	3.516×10^{-4}	.74
x_3x_4	1.756×10^{-4}	1	1.756×10^{-4}	.37
Error	4.772×10^{-3}	10	4.772×10^{-4}	
Total	9.758×10^{-1}	24		

*Significant at $\alpha = 0.10$

The remaining five terms (x_1, x_2, x_3, x_4, and x_2^2) represent a reduced but statistically adequate model of the true response surface.

The final response surface, consisting of four linear terms and one quadratic, to be used in the remainder of this DNBR analysis is given in Table 15. As before, the polynomial is listed in a vertical format. The table also gives the correspondence between the standardized variables and the physical variables of the analysis. The coefficient of multiple determination, R^2, for this final model is 0.9923.

Table 15

RESPONSE SURFACE MODEL FOR DNBR ANALYSIS

Coefficient	Variable	Definition of Variables
2.7043	1	
5.6191×10^{-2}	x_1	$x_1 = (P - 2250)/45$
-1.2256×10^{-1}	x_2	$x_2 = (T - 552.5)/5.525$
1.4939×10^{-1}	x_3	$x_3 = (G - 2.46 \times 10^6)/1.488 \times 10^5$
-8.8544×10^{-2}	x_4	$x_4 = (Q - 1.898 \times 10^5)/3.796 \times 10^3$
-1.4075×10^{-2}	x_2^2	

$R^2 = 0.9923$

VI. DETERMINATION OF THE DNBR PROBABILITY DISTRIBUTION

6.1 Monte Carlo Technique

Monte Carlo methods, in general, determine quantitative results regarding an estimate of the value of a multiple integral. In this analysis the multiple integral of interest consists of the probability that the local heat flux will not exceed the critical limit at which DNB occurs.

In order to estimate this probability by direct Monte Carlo procedures, the distributions of the input parameters of which the DNBR has been shown to be a function are randomly sampled. These selected values for the input are then propagated through the response surface chosen to represent the functional relationship between the computer code and the input variables. As the input selection and propagation procedure continues, a representative form of the DNBR distribution is established.

The accuracy of probabilities predicted from Monte Carlo-produced distributions are dependent upon the sample size.[15] When the probability of interest, p, is a very small number, which occurs when it is located in the tail of a distribution, the required sample size, n, is large. To estimate the accuracy of the estimate of

the probability for a given sample size, $\hat{p}_n$, the variance can be calculated by

$$\mathrm{Var}(\hat{p}_n) = \frac{p(1-p)}{n} \tag{27}$$

Thus, in order to estimate a probability of 10^{-4} to within ten percent of its value, a sample size of 10^6 is required.

Because of the large sample size requirement for the direct Monte Carlo technique, refined Monte Carlo methods have been developed which include some variance-reduction features and reduce the required sample size. For this analysis, however, due to the uncomplicated nature of the fitted response surface, the direct method was judged to be acceptable. It is also an efficient means of determining the mean and standard deviation of the DNBR distribution.

6.2 DNBR Distribution

In order to obtain a DNBR distribution, a direct Monte Carlo code was written and is included in Appendix D. In the code, values of the significant input parameters, selected in Chapter IV, are chosen from each respective normal distribution by means of normal random number selection developed by Box and Muller.[16] The DNBR is then evaluated at the specified input variables

by means of a fitted polynomial, developed in Chapter V, and partitioned for ease of interpretation.

The outcome from a direct Monte Carlo run with a sample size of 10^6 is shown in Figure 4, representing a minimum accuracy at 10% for probabilities down to 10^{-4}. This DNBR distribution gives an estimated mean value of 2.704 with a standard deviation of 0.110. A probability table as extracted from this distribution is given in Table 16. As can be seen by this table, the probability that the DNBR will be less than 2.125 is only 10^{-6}. This indicates a wide margin of assurance that the critical heat flux will not exceed the critical limit at which DNB would occur.

Figure 4

DNBR Distribution

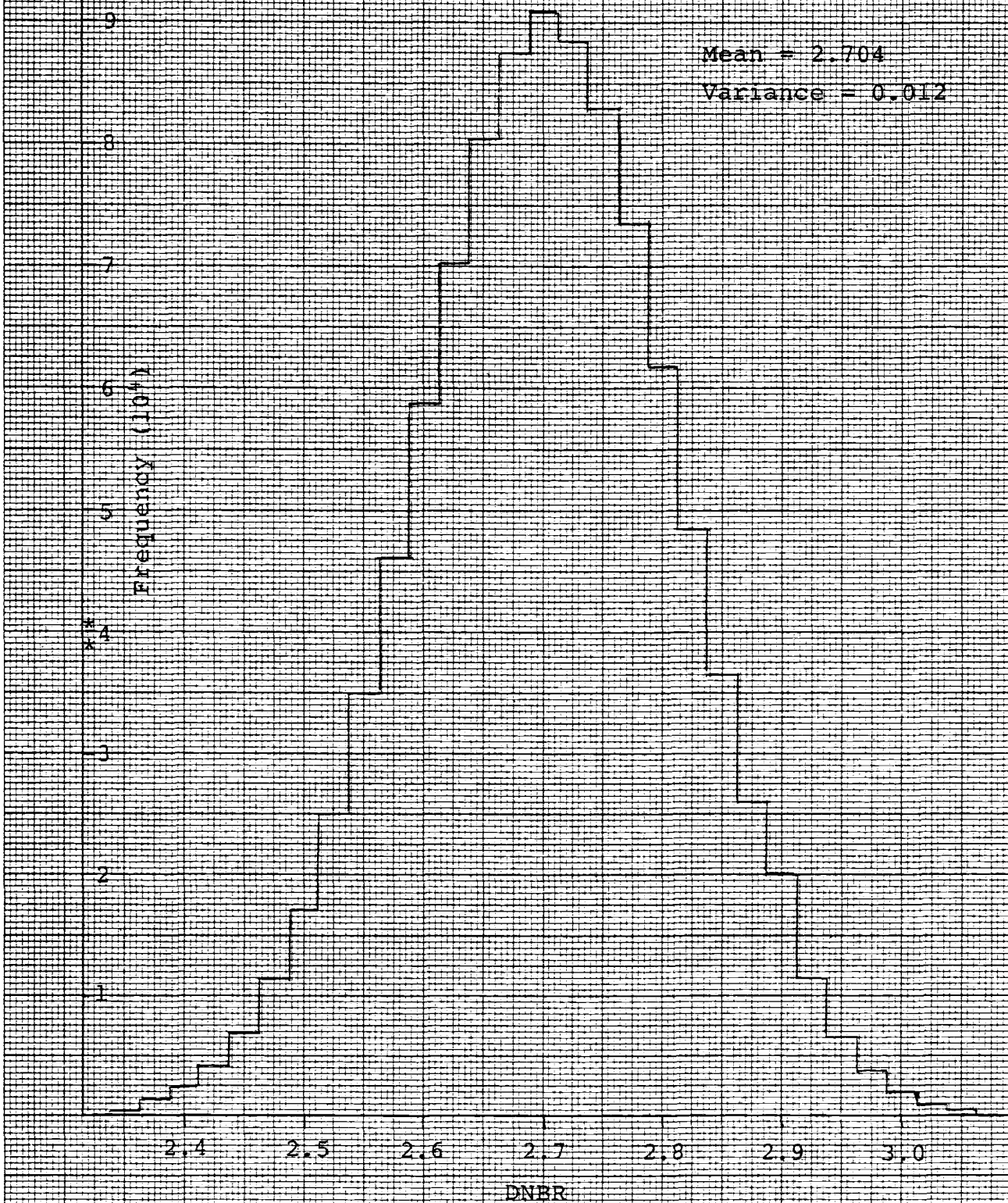

METRIC

Table 16

DNBR PROBABILITY TABLE

Reference DNBR (±.025)	Probability DNBR ≤ Reference DNBR
2.125	.000002
2.150	.000005
2.175	.000015
2.200	.000024
2.225	.000059
2.250	.000145
2.275	.000327
2.300	.000662
2.325	.00134
2.350	.00270
2.375	.00520
2.400	.00941
2.425	.0163
2.450	.0276
2.475	.0448
2.500	.0699
2.525	.105
2.550	.151
2.575	.210
2.600	.280
2.625	.361
2.650	.448
2.675	.539
2.700	.628
2.725	.710
2.750	.784
2.775	.846
2.800	.894
2.825	.931
2.850	.957
2.875	.974
2.900	.986
2.925	.992
2.950	.996
2.975	.998
3.000	.9992
3.025	.9997
3.050	.99986
3.075	.99995
3.100	.99998
3.125	.99999
3.150	.99999
3.175	1.00

VII. SUMMARY AND CONCLUSIONS

The assurance that departure from nucleate boiling (DNB) does not occur is an important basis for the design and operation of pressurized water reactors. In general, previous analyses of the departure from nucleate boiling ratio (DNBR), specifying the ratio of the heat flux at which DNB occurs to the local heat flux, have been deterministic and conservative. From these analyses it is difficult to assess the probability of attaining a critical value.

An alternative technique has been demonstrated in this analysis which results in a best-estimate calculation of the DNBR and its probability distribution. A computer code, COBRA IIIC/MIT, was used to perform the best-estimate calculation. Additional computer runs were made with the code to perform a sensitivity analysis on the code input variables in order to identify significant variables and minimize subsequent computational effort. With the less sensitive variables eliminated, the code was then used to evaluate the DNBR at selected combinations of the input values as prescribed by a central composite experimental design. Using the results of the design runs, a response surface was developed to simulate the computer code in subsequent

evaluations. The final estimate of the DNBR distribution was determined using a direct Monte Carlo technique in which input values were chosen at random from their respective distributions and propagated through the response function. From the resulting distribution it was demonstrated that, for the given conditions, the realistic probability of attaining a critical value of a DNBR was acceptably low.

For this analysis, a number of assumptions were made and therefore must be taken into account when considering the results. First of all, it is assumed that the DNBR is a function of only four significant parameters, each with uncertainty specified by a normal distribution with known means and standard deviations. It is also assumed that the deterministic relationship between the code inputs and the output as defined by the COBRA IIIC/MIT code is adequately represented by the fitted response surface. Any change made in these assumptions, either in the form of the initial input distributions or in the code, would alter the results and require a complete rerun of the Monte Carlo analysis. However, if the suitable approximating function does adequately represent the computer code, the statistical distribution for the DNBR is found by a means both inexpensive and efficient.

BIBLIOGRAPHY

1. Mazumdar, M., Marshal, J.A., and Chay, S.C., "Methodology Development for Statistical Evaluation of Reactor Safety Analysis," EPRI-NP-194, September 1975.

2. Bowring, Robert W. and Moreno, Pablo, "COBRA III/MIT Computer Code Manual," prepared for EPRI by MIT, March 1976.

3. Rowe, D. S., "COBRA IIIC: A Digital Computer Program for Steady State and Transient Thermal Hydraulic Analysis of Rod Bundle Nuclear Fuel Elements," BNWL-1695, March 1973.

4. Rowe, D. S. , "COBRA III: A Digital Computer Program for Steady State and Transient Thermal-Hydraulic Analysis of Rod Bundle Nuclear Fuel Elements," Interim Report, Battelle Pacific Northwest Laboratories, Richland, Washington, November 1972.

5. Masterson, Robert E. and Wolf, Tothar, "An Efficient Multidimensional Numerical Method for the Thermal-Hydraulic Analysis of Nuclear Reactor Cores," Nucl. Sci. and Eng., (64) pp. 222-236, 1977.

6. "Trojan Nuclear Power Plant Final Safety Analysis Report," Portland General Electric Company, Portland, Oregon.

7. Tong, L. S. , "Prediction of Departure from Nucleate Boiling for an Axially Non-uniform Heat Flux Distribution," J. Nucl. Energy, (21) pp. 241-248, 1967.

8. Levy, S., "Forced Convection Subcooled Boiling--Prediction of Vapor Volumetric Fraction," GEAP-5157, April 1966.

9. Ladieu, A. E., "A Thermal-Hydraulic Analytical Model Using COBRA IIIC," YAEC 1058, May 1974.

10. Chunis, J. A., "Connecticut Yankee Cycle V DNBR Sensitivity Study," NUSCO-114, September 1975.

11. de Stordeur, A. N., "Drag Coefficients for Fuel-Element Spacers," Nucleonics, (19), June 1961.

12. Cochran, W. G. and Cox, G. M., Experimental Design, 2nd Ed., John Wiley and Sons, New York, pp. 148-182, 1957.

13. Myers, R. H., Response Surface Methodology, Allyn and Bacon, Boston, pp. 127-134, 1971.

14. Neter, John and Wasserman, W., Applied Linear Statistical Models, Richard D. Irwin, Inc., Homewood, Illinois, pp. 214-272, 1974.

15. Kleijnen, J.P.C., Statistical Techniques in Simulation, Part 1, Marcel Dekker, Inc., New York, 1974.

16. Box, G. E. P. and Muller, M. E., "A Note on the Generation of Random Normal Deviates," Ann. Math. Stat., (29), pp. 610-611, 1958.

APPENDICES

APPENDIX A

NOMENCLATURE

a´.....Pressure gradient without crossflow in equation (7)

A.....Channel cross-sectional flow area

c.....Thermal conduction coefficient

C.....Crossflow resistance function

c_p.....Specific heat

D.....Hydraulic diameter, $4A/P_w$

f.....Friction factor based on all-liquid flow

f_h.....Fraction of power generated in fuel

f_p.....Flux spike peaking factor

f_t.....Turbulent momentum factor

f_{i-j}....Geometric fraction of heat from rod i which enters channel j

F_{i-j}....Overall fraction of heat from rod i which enters channel j

$F^E_{\Delta h}$.....Engineering enthalpy rise hot channel factor

F^E_q.....Engineering heat flux factor

g.....Gravitational constant

G.....Mass velocity

h.....Enthalpy, $Xh_g + (1 - X)h_f$

h´.....Heat transfer coefficient

h*.....Enthalpy carried by diversion crossflow

K.....Grid spacer loss coefficient

k.....Fluid thermal conductivity

k_f, k_c...Fuel and clad thermal conductivity, respectively

m.....Channel flow rate

N.....Number of rods in fuel region or temperature nodes

P.....Pressure

P_w.....Wetted perimeter

Pr.....Prandtl number

q'.....Heat addition per unit length

q''.....Heat flux

q'''.....Volumetric heat source density

Re.....Reynolds number

[S].....Matrix defining adjacent subchannels

$\frac{s}{\ell}$.....Turbulent momentum factor

t.....Time

t_c.....Cladding thickness

T.....Temperature

T_b.....Bulk liquid temperature

T_{sat}....Bulk saturation temperature

T_w.....Clad wall temperature

u.....Effective momentum velocity, mv'/A

u*.....Effective velocity carried by diversion crossflow

u''.....Effective velocity for energy transport

v.....Liquid specific volume

v'.....Effective specific volume for momentum,
$(1 - X)^2/\rho_f(1 - \alpha) + X^2/\rho_g\alpha$

w.....Diversion crossflow between adjacent subchannels

w'.....Turbulent crossflow between adjacent subchannels

x.....Distance

X.....Quality, $m_g/(m_g + m_f)$

α.....Void fraction, $A_g/(A_g + A_f)$

β.....Turbulent mixing factor, $w'/(G,D)$

γ.....Weighting function in equations (14) and (15)

θ.....Orientation of channel with respect to vertical

μ.....Nominal or mean parameter value

ρ.....Density of two-phase mixture, $\rho_g + \rho_f(1 - \alpha)$

ρ_f, ρ_c...Fuel and clad density, respectively

σ.....Standard deviation

ϕ.....Two-phase friction multiplier

Subscripts

f,g.....Saturation conditions for liquid and vapor, respectively

i,j.....Flow channel or fuel region identification number

ij,ji...Subchannel connection from i to j and j to i, respectively

f,c.....Fuel and clad properties, respectively

APPENDIX B

EQUATIONS FOR FUEL HEAT TRANSFER

To determine temperatures within the fuel, COBRA IIIC/MIT makes use of a heat transfer model developed by Rowe[3] which considers radial heat conduction. In this model, the fuel is divided into equally spaced concentric rings as illustrated in Figure 5. For N temperature nodes within the fuel, N + 1 temperatures are specified where the temperature at i = N + 1 is at the outer surface of the cladding.

The equations for the model are derived by approximating the heat conduction equation,

$$(\rho c_p)_f \frac{\partial T}{\partial t} = K_f\left(\frac{\partial^2 T}{\partial r^2} + \frac{1}{r}\frac{\partial T}{\partial r}\right) + q''' \qquad \text{(B-1)}$$

with a Taylor's series at each temperature node shown in Figure 5.

For the i = 1 node (r = 0), the boundary condition $\frac{\partial T}{\partial r} = 0$ can be applied. By using L'Hospital's rule, equation (B-1) becomes

$$(\rho c_p)_f \frac{\partial T}{\partial t} = 2K_f \frac{\partial^2 T}{\partial r^2} + q''' \qquad \text{(B-2)}$$

A Taylor's series can be used to express the nodal temperatures with respect to spatial and temporal change:

Figure 5

Fuel Heat Transfer Model

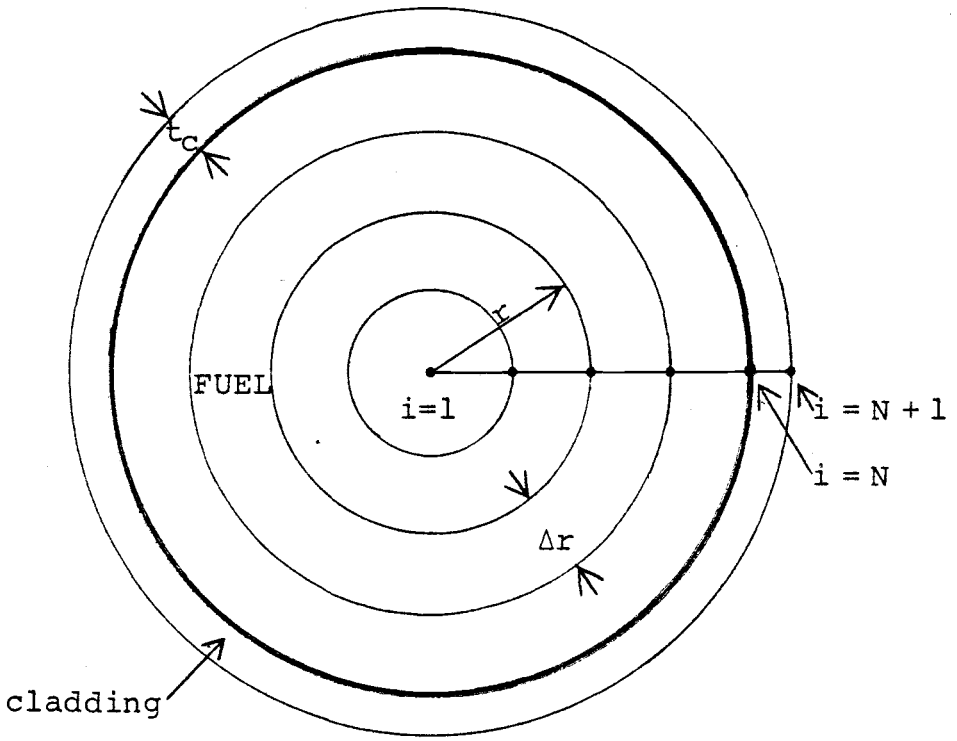

$$T_1 = \bar{T}_1 + \Delta t \frac{\partial T}{\partial t} + \ldots \tag{B-3}$$

$$T_2 = T_1 + \Delta r \underbrace{\frac{\partial T}{\partial r}}_{0} + \frac{\Delta r^2}{2!} \frac{\partial^2 T}{\partial r^2} + \ldots \tag{B-4}$$

where the overscore bar ($\bar{}$) denotes the temperature at a previous time step.

Neglecting higher order series terms and substituting these expansions into equation (B-2) produces a finite difference equation in the form of

$$(\rho c_p)_f \left[\frac{T_1 - \bar{T}_1}{\Delta t}\right] = 4K_f \left[\frac{T_2 - T_1}{\Delta r^2}\right] + q_1''' \tag{B-5}$$

where q_1''' represents the volumetric heat source in the $i = 1$ nodal volume.

For the interior fuel temperature nodes, $1 < i < N$, a similar procedure can be followed to obtain a set of $N - 2$ finite difference equations. A Taylor's series can be used to expand the local nodal temperatures

$$T_{i+1} = T_i + \Delta r \frac{\partial T}{\partial r} + \frac{\Delta r^2}{2!} \frac{\partial^2 T}{\partial r^2} + \ldots \tag{B-6}$$

$$T_{i-1} = T_i - \Delta r \frac{\partial T}{\partial r} + \frac{\Delta r^2}{2!} \frac{\partial^2 T}{\partial r^2} + \ldots \tag{B-7}$$

By adding equations (B-6) and (B-7), an expression can be found for the second derivative with respect to space

$$\frac{\partial^2 T}{\partial r^2} = \frac{T_{i-1} - 2T_i + T_{i-1}}{\Delta r^2} \qquad \text{(B-8)}$$

By subtracting the two equations, the first derivative can be written as

$$\frac{\partial T}{\partial r} = \frac{T_{i+1} - T_{i-1}}{2\Delta r} \qquad \text{(B-9)}$$

By defining r = (i - 1) Δr and substituting equations (B-8) and (B-9) into the heat conduction equation, a finite difference equation can be found which describes the interior fuel nodal temperatures.

$$(\rho c_p)_f \frac{T_1 - \overline{T}_1}{\Delta t} = K_f \frac{T_{i+1} - 2T_i + T_{i-1}}{\Delta r^2} + \frac{T_{i+1} - T_{i-1}}{2(i-1)\Delta r^2} \qquad \text{(B-10)}$$

At the i = N node, a fuel-clad interface condition

$$-K_f \left.\frac{\partial T}{\partial r}\right|_{i=N} = h_{gap}(T_N - T_{N+1}) \qquad \text{(B-11)}$$

can be applied. Here, an effective gap conductive coefficient is used which combines the conductance of the gap and cladding.

$$\frac{1}{h_{gap}} = \frac{1}{h_{\substack{gap \\ cond.}}} + \frac{t_c}{K_c} \qquad \text{(B-12)}$$

If equations (B-11) and the i = N expansion in equation (B-7) are used, equation (B-1) gives the finite difference equation

$$(\rho c_p)_f \left(\frac{T_N - \bar{T}_N}{\Delta t} \right) = 2K_f \left(\frac{T_{N-1} - T_N}{\Delta r^2} \right)$$

$$+ \left(\frac{2}{\Delta r} + \frac{1}{(N-1)\Delta r} \right) + h_{gap}(T_{N-1} - T_N) + q'''_N \qquad \text{(B-13)}$$

For determining the cladding temperature at i = N + 1, a transient heat balance for the cladding can be developed.

$$(\rho c_p)_c \left(\frac{T_{N+1} - \bar{T}_{N+1}}{\Delta t} \right) = \frac{h_{gap}}{t_c} \frac{r_N}{r_{N+1}} (T_N - T_{N+1})$$

$$- \frac{h'}{t_c} (T_{N+1} - T_b) + q'''_{N+1} \qquad \text{(B-14)}$$

where h′ is the surface heat transfer coefficient which is calculated by the heat transfer correlation.

In order to calculate the fuel temperature distribution, an implicit finite difference scheme is followed. Equations (B-5), (B-10), (B-13), and (B-14) which describe the nodal fuel temperatures can be rewritten. For the i = 1 node,

$$\frac{(\rho c_p)_f}{\Delta t^2} + \frac{4k_f}{\Delta r} T_1 - \frac{4k_f}{\Delta r^2} T_2 = q'''_1 + \frac{(\rho c_p)_f T}{\Delta t} \qquad \text{(B-15)}$$

For i = 2 to N - 1,

$$\left(-\frac{k_f}{\Delta r^2} + \frac{k_f}{2(i-1)\Delta r^2}\right) T_{i-1} + \left(\frac{(\rho c_p)_f}{\Delta t} + \frac{2k_f}{\Delta r^2}\right) T_i$$

$$+ \left(-\frac{k_f}{\Delta r^2} + \frac{k_f}{2(i-1)\Delta r^2}\right) T_{i+1} = q_i''' + \frac{(\rho c_p)_f \bar{T}_i}{\Delta t} \qquad \text{(B-16)}$$

For the i = N node,

$$\left(-\frac{2k_f}{\Delta r^2}\right) T_{N-1} + \left(\frac{(\rho c_p)_f}{\Delta t} + \frac{2k_f}{\Delta r^2} + \frac{2h_{gap}}{\Delta r} + \frac{h_{gap}}{(i-1)\Delta r}\right) T_N$$

$$+ \left(-\frac{2h_{gap}}{r} - \frac{h_{gap}}{(i-1)\Delta r}\right) T_{N+1} = q_N''' + \frac{(\rho c_p)_f \bar{T}_N}{\Delta t} \qquad \text{(B-17)}$$

For the i = N + 1 node,

$$-\left(\frac{h_{gap}}{t_c}\frac{r_N}{r_{N+1}}\right) T_N + \left(\frac{(\rho c_p)_c}{\Delta t} + \frac{h_{gap}}{t_c}\frac{r_N}{r_{N+1}} + \frac{h'}{t_c}\right) T_{N+1}$$

$$= q_{N+1}''' + \frac{(\rho c_p)_c \bar{T}_{N+1}}{\Delta t} + \frac{h'}{t_c} T_b \qquad \text{(B-18)}$$

These equations represent a set of N + 1 simultaneous equations for which the temperature coefficients represent a tridiagonal matrix. The solution of the temperature vector is accomplished by using a Gaussian elimination routine.

APPENDIX C

FRACTION OF POWER TO ADJACENT SUBCHANNELS

In general, the fraction of power to adjacent subchannels can be computed by knowing the geometry of the fuel rod and channel, the fraction of heat generated by the fuel, and the engineering hot channel factors. The geometry of the fuel rod or region and the flow channel determines the geometric fraction of the heat which enters the flow channel, f_{i-j}. The fraction of heat generated in the fuel, f_h, is included to maintain an accurate heat balance for the reactor. The engineering hot channel factors, $F^E_{\Delta h}$ and F^E_q, are included as uncertainty factors for the power distribution which affects the hot rod and the hot channel. They account for the influence of variations in the fuel pellet diameter, density, enrichment, pitch and bowing, the inlet flow distribution, and the flow mixing.

The equation for the overall fraction of heat from rod i to subchannel j, F_{i-j}, is dependent upon the type of fuel rod or region and channel. For energy transfer from the hot rod to the hot channel, this fraction is given by

$$F_{i-j} = f_{i-j} F^E_{\Delta h} / (f_h F^E_q f_p) \qquad \text{(C-1)}$$

The flux spike peaking factor, f_p, which is due to fuel densification is not usually included for DNBR studies but is shown for completeness. If this factor is included in the calculation, it is necessary to modify the code input by multiplying the hot rod relative power by this factor.

For power from a hot rod to a channel other than the hot channel, the overall fraction of heat transferred is written as

$$F_{i-j} = f_{i-j} / (f_h \, F_q^E \, f_p) \qquad \text{(C-2)}$$

The power from another rod to the hot channel can be represented by

$$F_{i-j} = f_{i-j} \, F_{\Delta h}^E / f_h \qquad \text{(C-3)}$$

For power from another rod to any channel other than the hot channel, the fraction of overall heat is

$$F_{i-j} = f_{i-j} / f_h \qquad \text{(C-4)}$$

For a lumped fuel region and channel, it is given by

$$F_{i-j} = N_i / f_h \qquad \text{(C-5)}$$

The fractions of power to adjacent channels shown in Table 7 were determined by the above equations. The

geometric fractions were obtained from Figure 2, and the fraction of heat generated in the fuel was assumed to be 0.974. The values for the engineering hot channel factors, $F_{\Delta h}^{E}$ and F_{q}^{E}, were taken to be 1.07 and 1.03, respectively.

APPENDIX D

MONTE CARLO SAMPLING CODE

```
      PROGRAM MONTE(INPUT,OUTPUT,TAPE1)
C
C          ************************************************
C          * VERSION 5     JULY 7, 1979    BY J. OYLEAR   *
C          * MONTE CARLO CODE FOR SAMPLING A DNBR RESPONSE *
C          * SURFACE                                      *
C          ************************************************
C
      DIMENSION XMEAN(4),SIGMA(4),X(4),N(40)
      DATA XMEAN/2250.,552.5,2.48E+06,1.898E+05/
      DATA SIGMA/22.5,2.7625,7.44E+04,1.898E+03/
      DATA N/17*0/
      PI=3.141592654
C
C          INPUT
C
      PRINT*,"ENTER NUMBER OF HISTORIES"
      READ*,NHIST
      PRINT*,"ENTER RANDOM NUMBER GENERATOR SEED"
      READ*,SEED
      CALL RANSET(SEED)
C
C          START SAMPLING DNBR RESPONSE SURFACE
C
      DO 20 J=1,NHIST
C
      DO 10 I=1,4
C
C          GENERATE UNIFORMLY DISTRIBUTED RANDOM NUMBERS.
C          RETURNS VALUE OVER RANGE (0,1) WITH ENDPOINTS
C          EXCLUDED. DUMMY ARGUMENT IS IGNORED.
C
      RN1=RANF(DUMMY)
      RN2=RANF(DUMMY)
C
C          DETERMINE RANDOM VALUES OF INPUT VARIABLES FROM
C          NORMAL DISTRIBUTION
C
      B=2.*PI*RN2
      A=SIGMA(I)*(-2.*ALOG(RN1))**.5
      RNKEY=RANF(DUMMY)
      IF(RNKEY.GT..5)GO TO 5
      X(I)=A*COS(B)+XMEAN(I)
      GO TO 10
 5    X(I)=A*SIN(B)+XMEAN(I)
 10   CONTINUE
```

```
C
C          TRANSFORM INPUT VARIABLES
C
      DO 15 K=1,4
      X(K)=(X(K)-XMEAN(K))/(2.*SIGMA(K))
 15   CONTINUE
C
C          CALCULATE DNBR FROM RESPONSE SURFACE POLYNOMIAL
C
      DNBR=2.7043+5.6191E-02*X(1)-1.2256E-01*X(2)+1.4939E-01*X(3)
     $-8.8544E-02*X(4)-1.4075E-02*X(2)*X(2)
C
C          PARTITIONING OF DNBR RESULTS
C
      IF(DNBR.GT.2.1875) GO TO 16
      WRITE(1,100) DNBR
      GO TO 20
 16   IF(DNBR.LT.3.2125) GO TO 17
      WRITE(1,100) DNBR
      GO TO 20
 17   DO 19 I=1,40
      C=2.1875+I*.025
      IF(DNBR.GT.C) GO TO 19
      N(I)=N(I)+1
      GO TO 20
 19   CONTINUE
 20   CONTINUE
C
C          OUTPUT
C
      DO 25 I=1,40
      WRITE(1,200) I,N(I)
 25   CONTINUE
C
C          FORMAT STATEMENTS
C
 100  FORMAT(F6.4)
 200  FORMAT(5X,"N(",I2,") = ",I7)
C
      STOP
      END
```